

Original Article

The disulfidptosis-related lncRNAs can predict survival and immunotherapy response accurately in endometrial carcinoma

Lin Hong^{1,2}, Ya-Xing Fang^{1,2}, Tao Li³, Yu-Feng He^{1,2}, Qin-Qin Jin^{1,2}, Xiao Xu^{1,2}, Shu-Guang Zhou^{1,2,4*}

¹ Department of Gynecology, Maternal and Child Health Center of Anhui Medical University, The Fifth Affiliated Clinical College of Anhui Medical University, Hefei, Anhui 230001, China

² Department of Gynecology, Hefei Maternity and Child Healthcare Hospital, Anhui Women and Children's Medical Center, Hefei, Anhui 230001, China

³ Department of Women's Health Care, Maternal and Child Health Institute of Anhui Province, Anhui 230001, China

⁴ Department of Gynecology, Linqun Maternity and Child Healthcare Hospital, Fu Yang, Anhui 236400, China

Article Info

Abstract



Article history:

Received: July 18, 2024

Accepted: January 23, 2025

Published: March 31, 2025

Use your device to scan and read the article online



Endometrial cancer of the uterine corpus (ECUC) is a common malignancy among females. Disulfidptosis, a recently identified form of cellular death, is characterized by elevated *SLC7A11* expression and limited glucose availability, making it a potential cancer treatment target. In this research, clinical data and transcriptome information from EC samples were accessed from the TCGA database. A disulfidptosis-related lncRNAs (DRLs) prognostic signature was developed by univariate/LASSO/multivariate regression analyses. Cellular pathways were identified through GO, KEGG, and GSEA analyses. Immune infiltration as well as tumor mutational burden (TMB) were evaluated. The TIDE algorithm and the GDSC database were utilized to predict how patients reacted to immunotherapy as well as anticancer drugs. Finally, the expressions of disulfidptosis-related lncRNAs were measured using *RT-qPCR*. Results: In this study, we identified 524 disulfidptosis-related lncRNAs and developed a prognostic signature consisting of five DRLs (*AC022960.1*, *PRDX6-AS1*, *EMSLR*, *AL359715.3*, *AC103563.9*). Our prognostic signature effectively stratified EC patients into high- and low-risk groups. Compared with the high-risk group, patients in the low-risk group exhibited better overall survival (OS). Additionally, ROC curves and concordance index (C-index) plots were used to assess the accuracy of our prognostic signature. The results demonstrated that the AUC values for 1-, 3-, and 5-year survival were 0.676, 0.712, and 0.722, respectively, indicating high predictive accuracy. Further analysis revealed significant differences between high- and low-risk groups in terms of TMB, drug sensitivity, and immune cell infiltration. *PCR* results showed that *PRDX6-AS1*, *EMSLR*, *AL359715.3*, and *AC103563.9* were upregulated in EC cells, whereas *AC022960.1* was downregulated. In conclusion, we developed a DRLs signature capable of predicting the TMB, prognosis, and immunological cell infiltration patterns, as well as the reactions to immunotherapy in EC patients.

Keywords: Disulfidptosis, Endometrial cancer, Immune landscape, Long non-coding RNA, Prognostic signature

1. Introduction

Endometrial cancer of the uterine corpus (ECUC) is one of the most widespread cancerous diseases among females worldwide; besides its incidence is rising globally [1, 2]. Annually, endometrial cancer is responsible for approximately 76,000 female fatalities. EC is a significant concern for women's health, particularly in industrialized nations, where its occurrence is highest due to both illness mortality and the increased number of newly diagnosed cases [3, 4].

Even though most early-stage EC patients can be cured by surgical treatment, advanced-stage patients are frequently treated by an amalgamation of chemotherapy, radiation therapy, and surgery. Despite this, the overall

survival and life quality for many EC patients remains suboptimal [5]. Therefore, identifying reliable EC-related biomarkers is crucial in order to use prognostic modeling to learn more about EC patients' prognosis evaluation and their responses to therapeutic interventions.

Transcripts longer than two hundred nucleotides, which do not encode proteins, are known as long non-coding RNAs (lncRNAs) [6]. Among the most prevalent regulatory elements inside the non-coding sections of the genes are loci that encode lncRNA [7]. Through their interactions with DNA, RNA, as well as proteins, lncRNAs are involved in the regulation of gene expression and protein function [8, 9]. Given their role in controlling the expression of genes in pathological settings, lncRNAs may be

* Corresponding author.

E-mail address: zhoushuguang@ahmu.edu.cn (S-G. Zhou).

Doi: <http://dx.doi.org/10.14715/cmb/2025.71.3.3>

associated with a wide variety of disorders [10]. Specifically, many researches have shown that lncRNAs exhibit distinct expression patterns, which are cell-state-specific, in terms of time, and spatially, therefore performing essential roles in tumorigenesis and tumor progression[11]. In addition, an increasing number of researches have shown that lncRNAs accelerate the progress of EC [12-14].

Dysregulation of cell death, a fundamental process that is essential to many biological functions, is closely associated with the onset and the course of many diseases [15]. Liu discovered a novel type of cellular death, termed Disulfidptosis, in February 2023. According to the researchers, the overabundance of intracellular cystine buildup caused disulfide stress, which subsequently induced the death of cells. Disulfide accumulation disrupted the typical relationship amid cytoskeletal proteins in cancer cells, which overexpress *SLC7A11* and are glucose-deficient, ultimately leading to the collapse of the histone death of cells and skeleton[16].

In our research, we have created a prognostic signature for endometrial carcinoma Disulfidptosis Related Long Non-Coding RNAs (DRLs). Our approach used TCGA-UCEC cohort in order to comprehend different aspects of endometrial cancer, including mutation, immunological state and chemotherapeutic drug response. Patients' information mined from publicly accessible datasets was part of our research, and it was followed by a thorough analysis that included immunology enrichment, and medication-sensitive evaluation. Furthermore, we carried out internal experimental validation to confirm the exceptional dependability and stability of our signature. This thorough method provided an innovative viewpoint on the application of precise and personalized methods of treatment for tumor management. The one using a potent framework for improving our knowledge of endometrial cancer and directing specialized therapeutic actions for better patient outcomes is offered by advanced medical big data. Overall, our research contributes significant novel and scientific worth to the care of patients with EC, advancing the field in tumor immunology.

2. Material and methods

2.1. Acquisition and Pre-processing of data

Transcriptomic data based on RNA sequencing, clinical details as well as mutational data came from The Cancer Genome Atlas (TCGA) database, UCEC project (access time 17 October 2023). After being downloaded in a "STAR-Counts" form, each EC patient's expression profiles were obtained and added to a merging matrix. Similarly, EC patient's clinical information was downloaded in "BCR-Xml" form. Making use of the R code, all of the data were acquired and sorted out. The dataset included 554 EC tumor cases and 35 normal controls. Normal specimens were not included in further examinations. Samples of EC patients lacking appropriate details on age, tumor stage, and survival time were likewise eliminated. Finally, we acquired 543 EC samples. The experimental design flowchart for our research is displayed in Figure 1.

2.2. Finding DRLs

Based on earlier researches, we were able to identify ten disulfidptosis-related genes (DRGs), comprising *RPNI*, *NCKAP1*, *NDUFA11*, *LRPPRC*, *NUBPL*, *NDUFS1*, *GYS1*, *SLC7A11*, *SLC3A2*, and *OXSM*[16]. The DRGs were

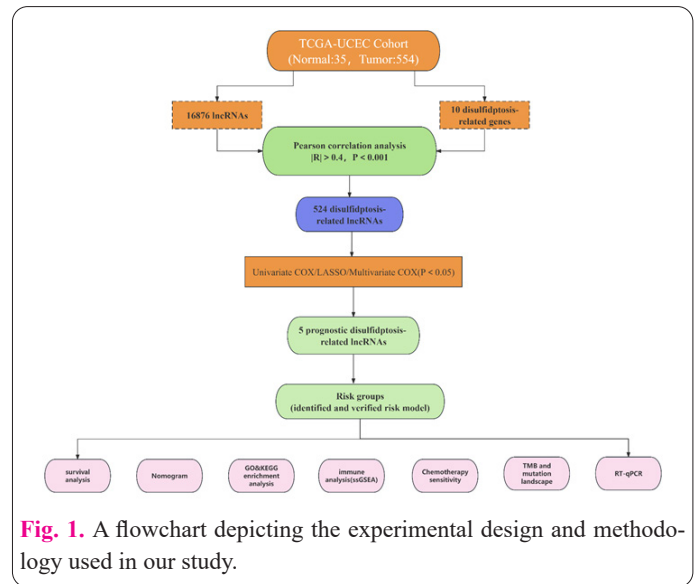


Fig. 1. A flowchart depicting the experimental design and methodology used in our study.

screened for co-expression patterns with lncRNAs using Pearson correlation analysis, with a threshold of $p < 0.001$ as well as a correlation coefficient absolute value greater than 0.4. DRLs are the definition given to these lncRNAs.

2.3. Creation and verification of a DRLs signature

A total of 543 cases with survival information were randomly divided into two groups: the training group ($n = 272$) was utilized for the model's development, and the testing group ($n = 271$) was employed to verify our signature. DRLs were identified by Univariate Cox Regression Analysis. Notably, these DRLs were strongly associated with patients' OS in training cohort. Finding the lncRNAs with the least amount of divergence follows LASSO Regression Analysis, and a prognostic model derived from five DRLs was created by Multivariate Cox Regression Analysis. Each of the five DRLs' expression values as well as regression coefficient were added up to create the risk score via employing following equation: Risk Score=

$$\sum_{i=1}^n \text{Expression (LncRNA)} * \text{Coefficient (LncRNA)}$$

Patients' medium-risk score was exploited to categorize them into groups with different risks. For the purpose of assessing the significance of our predictive model, then we performed survival analysis. The testing group's samples were then utilized to verify the prognostic signature's accuracy. In order to ascertain whether our risk score obtained based on constructed model acts as an independent prognostic factor across different samples, an investigation of multifactorial analysis was carried out.

2.4. Functional enrichment

Following screening criteria were utilized in order to acquire differentially expressed genes (DEGs) among distinct categories: A filtering criteria of false discovery rate (FDR) < 0.05 as well as \log_2 fold change absolute value greater than 1. To learn more about potential molecular mechanisms, which differentiate across the groups at different risk, pathway studies such as Gene Ontology (GO) as well as Kyoto Encyclopedia of Genes and Genomes (KEGG) analyses were carried out. When the $FDR < 0.05$, GO or KEGG pathways were deemed substantially enriched. Focusing on GO gene sets and based on the gene expression disparities across the groups at different risks, Gene Set Enrichment Analysis (GSEA) then was studied

as well. When a gene set's p value < 0.05 , it will be deemed enriched.

2.5. Tumor-infiltrating analysis of immune cells

Gene expression data were analyzed using the ESTIMATE algorithm to assess the abundance of both immune and stromal cells in EC tissues [17]. Grounded in a single sample GSEA (ssGSEA), the ESTIMATE algorithm generated three scores including stromal scores, immunological scores, as well as estimate scores, which is the sum of the previous two scores. These scores were used to compare variations across the different risk groups. The CIBERSORT tool [18] was utilized to evaluate the 22 immune cell types' abundances in each EC sample. Additionally, each sample's various immune functions were assessed using a ssGSEA employing gene sets related to immunity, and the two groups' immune functional activities were compared.

2.6. Tumor mutation analysis

We obtained TMB data for EC patients from the TCGA database. TMB was quantified as the total number of mutant bases per million bases. To investigate the effect that TMB has on overall survival in different cases, patients were divided into different groups given the median score on TMB, and survival analysis then was implemented for each group. For the intention of studying the mutation profiles in more detail, we employed R package "MAF tool" [19] to assess and render the fifteen most frequently mutated genes in tumors in EC samples within the database. This analysis highlighted genes with a higher frequency of mutations. We also conducted log-rank tests for analysis of survival and evaluated TMB levels across the different categories. We sought to investigate the potential influence of TMB concerning EC patients' prognosis by assessing TMB's correlation with patient survival.

2.7. Immunotherapy response and drug sensitivity prediction

To forecast how EC patients would react to immunotherapy, Tumor Immune Dysfunction and Exclusion (TIDE) studies were carried out. Considering the immunological microenvironment of the tumors. The TIDE score is a computational method that evaluates the potential for

immunotherapy response. The response to immunotherapy is inversely correlated with TIDE prediction scores. By contrasting the TIDE scores, it was possible to determine how differently patient categories at high and low risk responded to immune therapy. Furthermore, to forecast EC patients' susceptibility to widely used chemotherapy drugs, we used the R package "oncoPredict" [20]. The half-maximal inhibitory concentration (IC50) values of EC samples were acquired based on the Genomics of Drug Sensitivity in Cancer (GDSC) database used in this package [21]. Through evaluating the IC50 values, we successfully predicted the EC patients' varying chemosensitivity to several chemotherapeutic drugs that are often used in clinical work.

2.8. The Cell Culture and RT-qPCR

We employed a variety of cell lines in our experimental investigation, including *Ishikawa* and *HEC-1-A* endometrial malignancy cells and normal endometrial cells from *HEEC*. These cells were procured via the American Type Culture Collection (ATCC), and cultivated in F-12, Leibovitz's L-15 medium (Gibco BRL, USA), or McCoy's 5A. Total cell RNA was taken out of cell lines utilizing 10% fetal bovine serum (Gibco BRL, USA) in a 95% humidity, 37°C, and 5% CO₂ cell culture using a standard protocol-based extraction reagent for total RNA (10606ES60, YEASEN). After that, the produced RNA was employed to synthesize cDNA in the cDNA synthesis kit (11139ES10, YEASEN). The expression of genes was measured using SYBR green premixed solution (11201ES03, YEASEN) using Roche photo cycler 480 and 2- $\Delta\Delta C_t$ technique. *GAPDH* acts as an interior standard for uniformity. Every primer used in RT-qPCR is produced by subcarriers (Shanghai subcarriers). Table 1 contains five primer sequences that are employed in PCR process for your reference.

2.9. Statistical analysis

R software (version 4.3.1) was applied in our study to analyze all data. Student's t -tests were applied to analyze data distinctions across the groups. For survival analysis, the Kaplan-Meier assessment as well as the log-rank test were both applied. If the p -value was < 0.05 , then differences across the two groups were considered to have sta-

Table.1. Five primer pairs sequences that were employed in PCR process.

DRLs	Sequences
PRDX6-AS1-Forward	5'- CAAGCTGGCTGTTTGAATGA-3'
PRDX6-AS1-Reverse	5'-CAAGCTGGCTGTTTGAATGA-3'
AC022960.1- Forward	5'- CAGCAGTAGGAGCTACCTGTGTC-3'
AC022960.1-Reverse	5'- ATAGAAGGGCATGACTGGCGG-3'
EMSLR-Forward	5'- TTCACACTTGCAGCAGATCC-3'
EMSLR-Reverse	5'- CTTTTTCACGTTTCCCGTGT-3'
AL359715.3-Forward	5'-ATCACTCTGAGAGGGCCCAAC-3'
AL359715.3-Reverse	5'- AGGCCTCAGACCCACGAAGAA-3'
AC103563.9-Forward	5'-AAGGTGTGACTTTACATCGAACGCC-3'
AC103563.9-Reverse	5'-CGCAGACAGGAGCGTTAGAATTGAG-3'

tistical significance for the above analyses.

3. Results

3.1. Identification of DRLs

RNA sequencing data for patients with EC was obtained from TCGA. lncRNAs and mRNAs were identified based on gene type annotation. To determine which lncRNAs are involved in disulfidptosis, Pearson correlation analysis then was employed based on the expressions of lncRNAs as well as 10 DRGs. Adhering to strict screening standards: P value < 0.001 as well as Pearson R absolute value greater than 0.4, we have acquired 524 DRLs. Eight of the ten DRGs had a correlation with the expression of these DRLs (Figure 2A).

3.2. Development of the DRLs signature

A total of 543 EC cases possessed survival data and were divided into two different groups at random, the test group was used for model validation, whereas the construction of model was done with the training group. From among the 524 DRLs, for the purpose of building the model, only those associated with the survival of EC patients were taken into consideration. Eighteen DRLs remained after we employed Univariate Cox regression analysis by excluding lncRNAs which did not significantly affect survival. Among these lncRNAs, one lncRNA was positively correlated with prognosis, but the remaining lncRNAs were negatively associated (Figure 2B). Using those 18 survival-associated DRLs and utilizing LASSO Cox regression analysis as well as Analysis of Multivariate Cox regression, a signature comprising five DRLs was established further (Figure 2C,2D). Subsequently, we determined every patient's risk score using the prognostic model equation: Risk score = $(0.992995785598745) * PRDX6-AS1 + (-2.23052913447989) * AC022960.1 + (0.41533950980956) * EMSLR + (0.5439915993848869) *$

$AL359715.3 + (0.972275688297637) * AC103563.9$. The correlations of expression across the five DRLs and ten DRGs are displayed in Figure 2E. *AC103563.9* and *EMSLR* revealed positive correlations. However, *AC029960.1* had negative relationships with the majority of DRGs. As expected, using the central risk quotient as a guide, patient data were classified into cohorts of different risks. A less favorable prognosis was corroborated by Kaplan-Meier plots, which displayed that individuals belonging to the layer of high-risk scores possessed lower OS compared with their counterparts in the category of low-risk. An upsurge in the death rate of the samples was associated with higher risk scores whether in the train set or test set. Additionally, the heatmap illustrated, particular lncRNAs such as *PRDX6-AS1*, *EMSLR*, *AL359715.3*, and *AC103563.9* were predominantly upregulated in the category of high risk. Nevertheless, *AC022960.1* was primarily upregulated in the lower-risk category (Figure 3A-C).

3.3. DRLs signature predicts survival of endometrial carcinoma

Next, we investigated whether any additional clinical characteristics could influence our predictive model. We enlisted three clinical characteristics of EC patients, such as age, grade as well as risk score in further studies. Univariate analysis revealed age (HR: 1.032, 95% CI: 1.011–1.054, $p < 0.05$), five DRLs-based risk scores (HR: 1.181, 95% CI: 1.096–1.273, $p < 0.001$) and tumor grade (HR: 2.605, 95% CI: 1.814–3.740, $p < 0.001$) are three risk variables that affecting prognosis (Figure 4A). Additionally, the Multivariate regression analysis indicated that risk score (HR: 1.096, 95% CI: 1.008–1.190, $p < 0.05$), age (HR: 1.025, 95% CI: 1.003–1.047, $p < 0.05$), grade (HR: 2.303, 95% CI: 1.589–3.338, $p < 0.001$), are independent prognostic variables (Figure 4B). Both ROC curves as well as C-index plots were employed to examine the precision of these risk score signatures. For 1, 3, and 5 years,

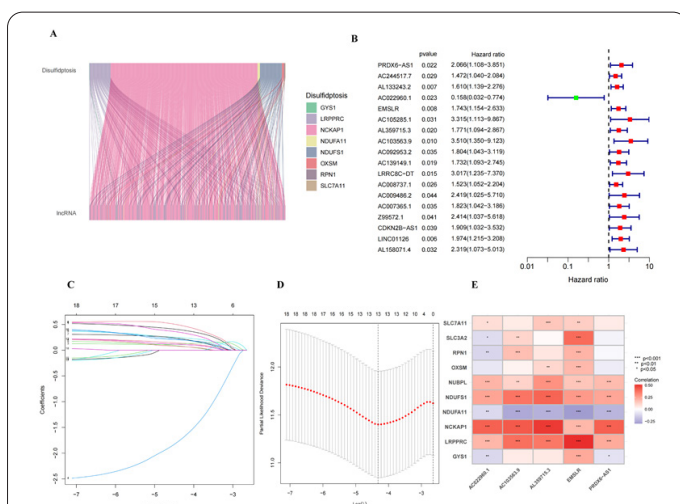


Fig. 2. Identification of DRLs and the establishment of a prognostic model for predicting overall survival in EC patients. (A) The Sankey graph reveals expression correlations between 8 DRGs and 524 DRLs. (B) Univariate Cox regression analysis reveals DRLs that impact EC patients' overall survival. (C) DRLs' LASSO coefficients. (D) The dotted lines in the LASSO regression represent the optimum $\log(\lambda)$ value. (E) The heatmap reveals the expressed correlations among the DRGs and the five DRLs utilized in the creation of the model. *, $p < 0.05$; **, $p < 0.01$; ***, $p < 0.001$.

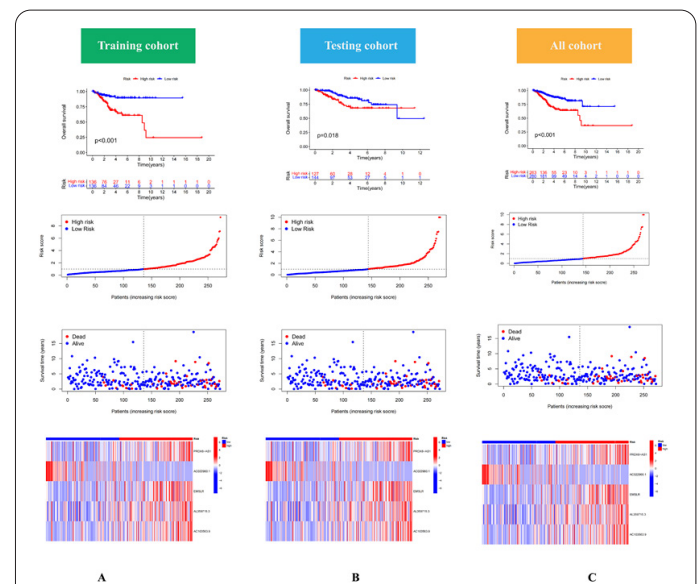
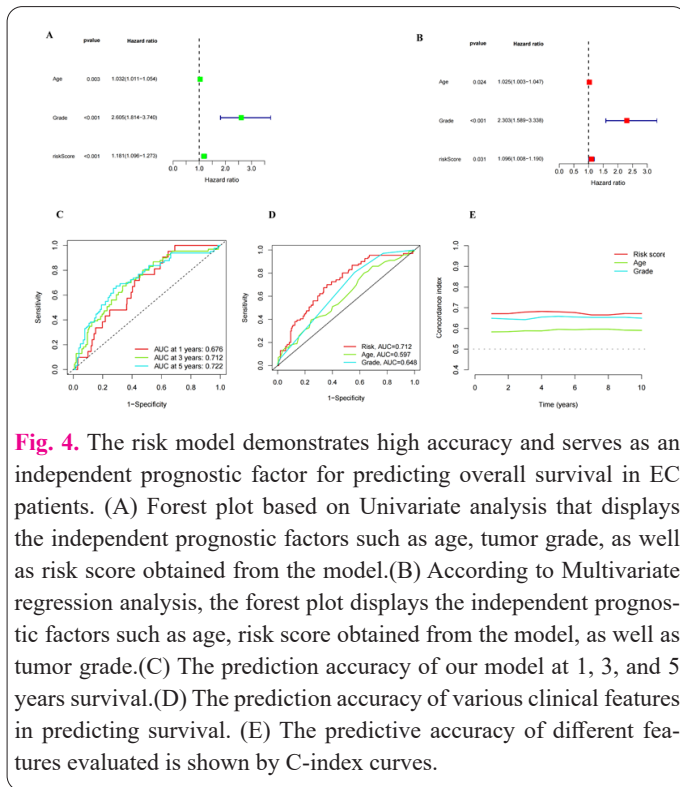


Fig. 3. Evaluation of the prognostic value of the risk model across the training, testing, and entire patient cohorts. (A) Kaplan-Meier plot shows that there is a relationship between survival time and different risk scores (top). Scatter plot displays how the survival time and risk score are related (middle). The heatmap shows the five DRLs' expressions among various risk categories (bottom). (B, C) Testing and the total datasets went through the same process.



the AUC values were 0.676, 0.712, and 0.722 respectively (Figure 4C), suggesting high accuracy of our prognostic model. Moreover, ROC curves were used to evaluate the risk score's forecast accuracy derived from model. Compared to the AUCs for grade (0.648) and age (0.597), the risk score's AUC (0.712) was higher (Figure 4D). The superior accuracy of our risk model in relation to age and grading criteria was further confirmed by C-index plots (Figure 4E). The results indicated that we developed a model, which can function as a reliable and independent prognostic signature.

3.4. Nomogram and Clinicopathological features

To improve the prognostic model's prediction capacity of EC patients, a nomogram was developed using risk scores as well as other clinical features (age, grade) of 543 EC samples. This nomogram was designed to estimate the predicted survival durations at 1, 3, and 5 years for EC patients (Figure 5A). The calibration chart shows a strong alignment between expected and observed results (Figure 5B). Next, we examined survival differences in Progression-Free Survival (PFS) across different groups by K-M curves. These outcomes showed that ECs in the group at low risk outlived those patients in the category of high risk in PFS (Figure 5C). In various age and grade categories, the variations in OS across the different groups were further examined (Age \leq 65 and Age $>$ 65), early grade group (grade 1 and 2) and advanced grade group (grade 3 and 4) (Figure 5D-G). The findings indicated that the predict model with a high degree of prediction accuracy and might be utilized for comparing patient survival across various groups, including age as well as tumor grade.

3.5. Principal Component Analysis (PCA)

We performed PCA based on each sample's risk score to ascertain whether patients at different risk levels could be distinguished. Considering the expression profiles' dimension variables of the entire genome, 10 DRGs, 524 DRLs,

as well as the risk score model. Four distinct PCA graphs are displayed in Figure 6. Our study outcomes indicated that from our risk score model's PCA graph, conspicuous differences exist in how the different risk score categories are distributed, specific clusters were present in both of the groups as well, unveiling that our model is effective in categorizing EC patients.

3.6. Immune regulation involving the DRLs signature

Using differentially expressed gene analysis, we were able to identify 441 DEGs among the categories at different risks, providing further insight into the biological differences between them. By carrying out biological mechanisms such as GO as well as KEGG pathway analyses, we clarified the differentially expressed genes (DEGs) bio-

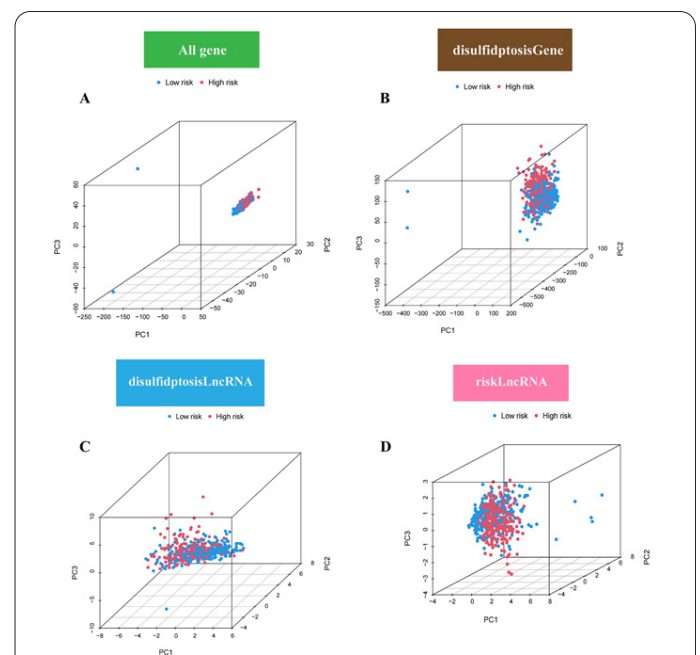
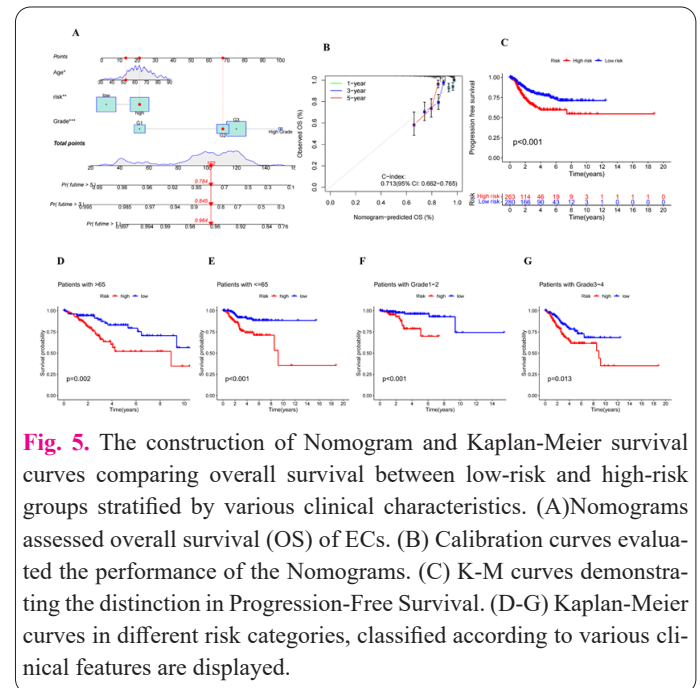


Fig. 6. The results of PCA analysis comparing the low- and high-risk cohorts of EC patients. (A) Principal component analysis (PCA) profiles of all genes. (B) PCA profiles of DRGs. (C) PCA profiles of DRLs. (D) The PCA profiles of DRLs used in the model.

logical mechanisms and processes in the different risk categories. As shown by the GO analysis, DEGs were mostly linked to physiological mechanisms such as pattern specification process, regionalization, and axon development. In point of cell localization, DEGs were primarily focused in areas such as the cell body of neurons and extracellular matrix containing collagen. At the molecular level, DEGs were chiefly involved in receptor-ligand activity (Figure 7A-D). In the context of KEGG pathway enrichment studies, DEGs were principally associated with the control of Neuroactive interaction of ligand-receptor, cell adhesion molecules, and Wnt signaling pathway (Figure 8A,8B). Consequently, we guessed that disulfidptosis might be connected to cancer metastasis and immunological mechanisms. Additionally, transcriptome-inclusive GSEA was performed. Our study demonstrated that Chromosome segregation, DNA replication, DNA templated, Nuclear chromosome segregation, and Regionalization are the five most highly enriched terms within the category of elevated risk, but within the low-risk group, Axoneme assembly, immunoglobulin complex, circulating immunoglobulin complex, immunoglobulin receptor binding, and antigen-binding are the top 5 cellular processes that are considerably enriched(Figure 8C,8D).Tumor immune microenvironment is a major factor in determining how quickly a tumor progresses. Taking into account the GSEA values above, which indicated that immunological regulation-related functions were enriched within those at low risk, therefore we hypothesized that the TME differs in certain ways across EC groups at diverse risk. On the basis of the ESTIMATE algorithm, compared with those individuals who belonged to low-risk, the immunological scores in the elevated-risk group are much lower (Figure 9A), suggesting that immunological cell infiltration degree is lower among groups of high-risk. Next, we utilized CIBERSORT method to examine the distribution level of distinct kinds of immunological cells within the tissues of EC patients. Exactly as demonstrated in (Figure 9B,9C), groups with high risk possess less penetration of regulatory T cells,

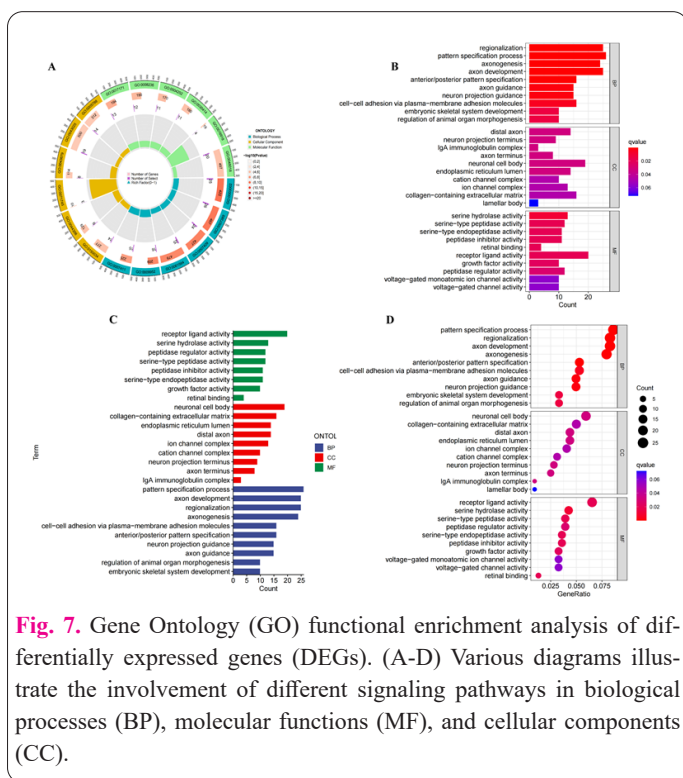


Fig. 7. Gene Ontology (GO) functional enrichment analysis of differentially expressed genes (DEGs). (A-D) Various diagrams illustrate the involvement of different signaling pathways in biological processes (BP), molecular functions (MF), and cellular components (CC).

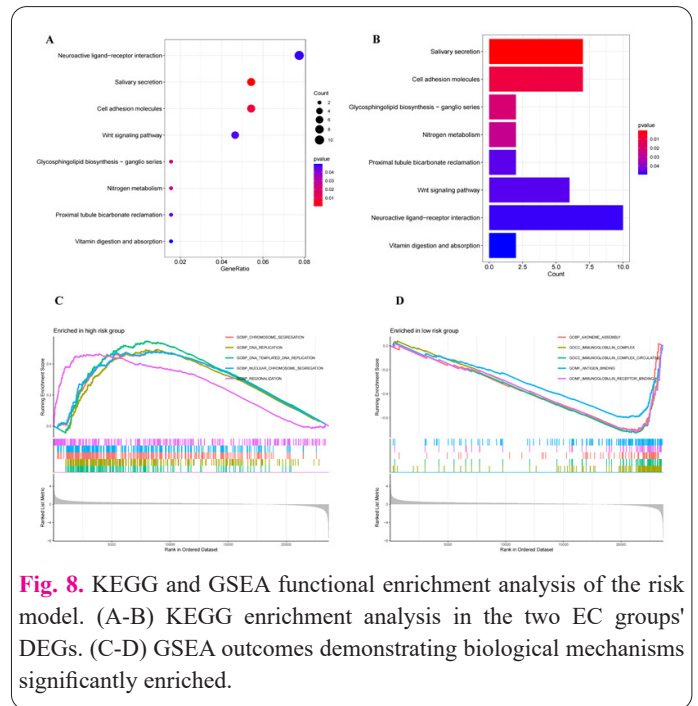


Fig. 8. KEGG and GSEA functional enrichment analysis of the risk model. (A-B) KEGG enrichment analysis in the two EC groups' DEGs. (C-D) GSEA outcomes demonstrating biological mechanisms significantly enriched.

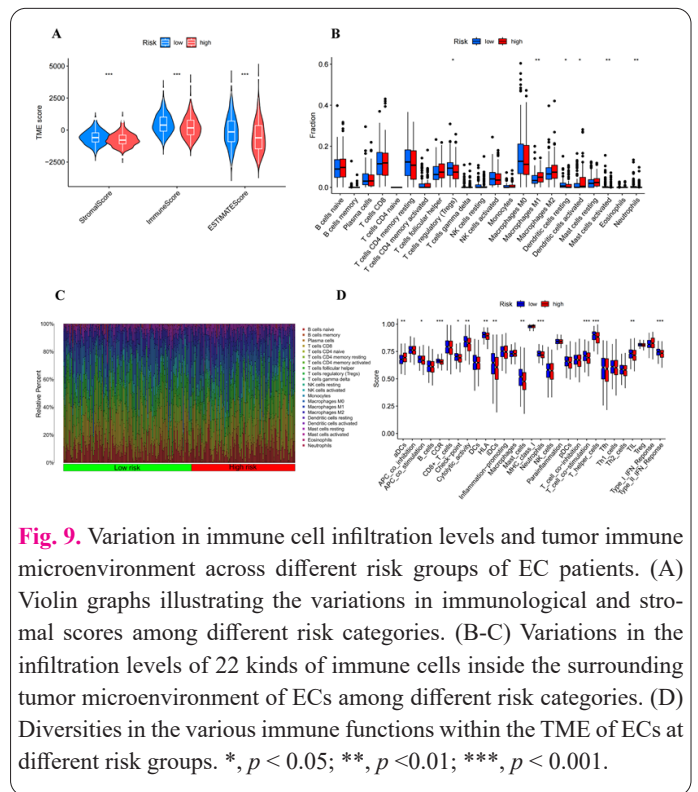


Fig. 9. Variation in immune cell infiltration levels and tumor immune microenvironment across different risk groups of EC patients. (A) Violin graphs illustrating the variations in immunological and stromal scores among different risk categories. (B-C) Variations in the infiltration levels of 22 kinds of immune cells inside the surrounding tumor microenvironment of ECs among different risk categories. (D) Diversities in the various immune functions within the TME of ECs at different risk groups. *, $p < 0.05$; **, $p < 0.01$; ***, $p < 0.001$.

Neutrophils, and Macrophages M0, but greater penetration of Macrophages M1. Furthermore, we examined a variety of immunological activities in the two groups. Notably, out of the 29 distinct immune function types, 21 exhibited reduced function scores among cohorts at higher risk than those at lower risk, including TIL, T helper cells, as well as cytolytic activity (Figure 9 D). In sum, our findings elucidated that in the groups with high risk, as categorized by DRLs signature, possibly have compromised immunological reactions in the tumor microenvironment, which could facilitate cancer metastasis and contribute to poorer overall survival.

(DEGs). (A-D) Various diagrams illustrate the involvement of different signaling pathways in biological processes (BP), molecular functions (MF), and cellular com-

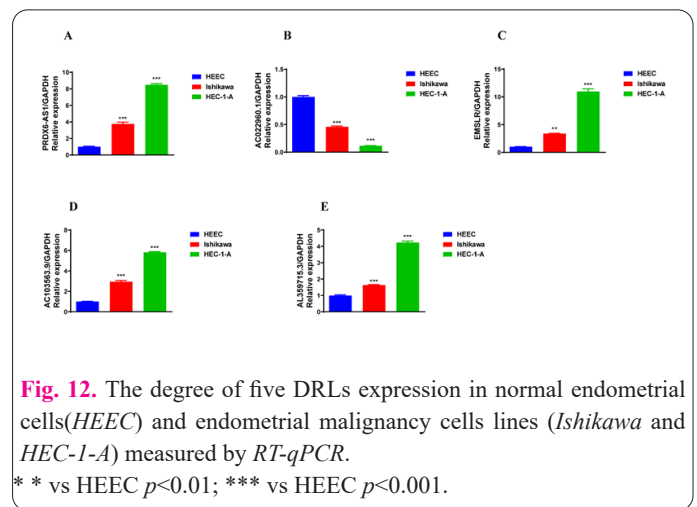
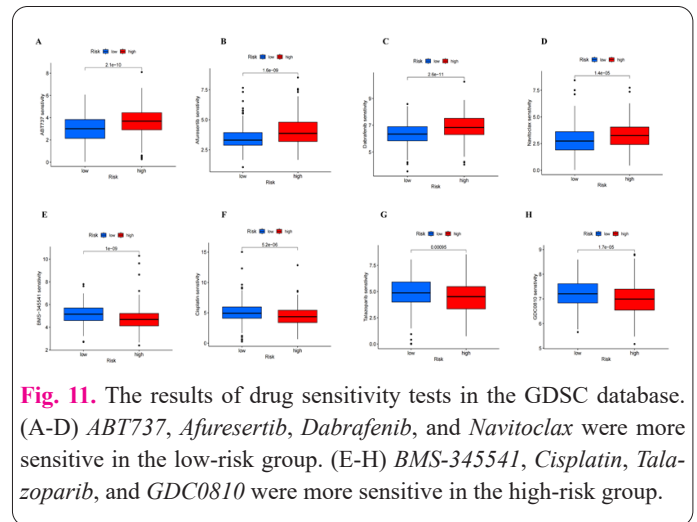
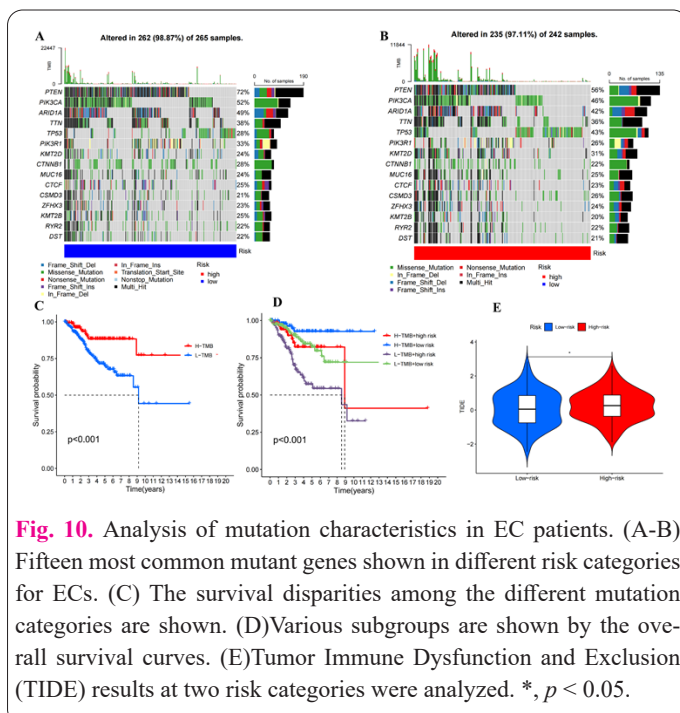
ponents (CC).

3.7. Somatic mutation landscape analysis

For many solid tumors, TMB, the quantity of somatic mutations found in each genomic mega base has the potential to be a prognostic biomarker. Gene mutation frequency and TMB were examined and compared across the two groups. The waterfall graphic provides insight into the frequency of the top 15 somatic gene mutations, indicating an increased mutation frequency within low risk individuals as opposed to that who at high-risk (Figure 10A,10B). Next, we studied how TMB combined with risk score affect the OS of ECs; these two criteria were used to separate the patients into four subgroups. Our study showed that compared to lower TMB levels, higher TMB levels were associated with improved overall survival (OS) (Figure 10C). It was discovered that individuals with elevated TMB as well as lower risk scores displayed the optimal prognosis. However, in contrast, individuals with high-risk scores and diminished TMB have the poorest prognosis (Figure 10D). At last, to evaluate the correlation across risk categories and immunotherapy response, the TIDE algorithm was utilized. The findings showing that samples at high risk might be more likely to avoid immunization, which may cause a worse reaction to immune therapy (Figure 10E).

3.8. Drug sensitivity response analysis

To explore the potential effectiveness of immunotherapy in EC patients and the possibility of dose modification, we analyzed the sensitivity of various immunotherapeutic drugs in relation to the risk score. Utilizing "OncoPredict" package, we estimated the half-maximal inhibitory concentration (IC50) of some medications for each sample and contrasted the risk groups' medication sensitivity. Considering the differences in immunological landscapes, mutational patterns, and prognostic outcomes among various risk groups of patients with EC, we performed targeted medication screening, to determine the most effective treatment options for each group. The



results demonstrated that *ABT737*, *Afuresertib*, *Dabrafenib*, and *Navitoclax*'s IC50 results among the groups of low risk were lower (Figure 11A-D), showing that EC patients among the lower risk category would gain greater advantages from these medications during their treatment. Conversely, among those at high risk, the IC50 values of *BMS-345541*, *Cisplatin*, *Talazoparib*, and *GDC0810* were lower (Figure 11E-H), indicating that higher-risk ECs will be more susceptible to those medications. These findings suggest that our model could be a valuable tool for predicting how EC patients will respond to immune checkpoint blockers (ICBs) and other widely used antitumor agents.

3.9. DRLs expression by RT-qPCR

In order to confirm our model's dependability, we carried out *RT-qPCR* tests in EC cell lines to ascertain the five DRLs' expression levels. We carried out *RT-qPCR* in normal endometrial cells in humans (*HEEC*) and endometrial carcinoma cells (*HEC-1A* and *Ishikawa*). Our outcomes demonstrated that the expression degree of *AC022960.1* was down-regulated in EC cells in contrast to normal *HEEC* (Figure 12B). However, *PRDX6-AS1*, *EMSLR*, *AL359715.3*, *AC103563.9* were up-regulated in EC cells (Figs.12A, 12C, 12D). These findings support the validity of the risk model built using DRLs.

4. Discussion

A malignant tumor derived from the endometrial epithelium, uterine corpus endometrial cancer has become increasingly prevalent worldwide on account of incidence

rate and fatality rate [22]. Although surgical therapy is curative for people with early-stage uterine corpus endometrial cancer, 10-15% of patients present to the clinic having advanced in their disease, and their overall 5-year survival rate is a dismal 17% [3]. The rate of survival and life quality for the vast majority of EC cases are insufficient, despite the fact that most early instances can be treated with surgical treatment and advanced-stage cases are frequently cured with a combined effort of chemotherapy, radiation therapy, and surgery [5]. There exists a causal correlation between the progression of tumors and the escape of cellular death, which is regarded as a hallmark of cancer [23, 24]. According to recent researches, disulfidptosis is a particular kind of cellular death. *SLC7A11* expression is highly expressed in most cancerous cells, and they rely heavily on glucose for the synthesis of glutathione, which helps the cells fend off death. Thus, when the glucose transporter proteins are inhibited using GLUT inhibitors, they may result in the buildup of disulfides in cancerous cells; cause cytoskeleton disruptions, like intracellular actin; cause disulfidptosis to develop in such a manner but not spare the healthy cells, which could become a focus for cancer treatments in the future [16]. Given that cancer cells are susceptible to disulfidptosis, a potential therapeutic approach for treating cancer treatment could involve focusing on this recently discovered form of cell death. A disulfidptosis-based signature can forecast the prognosis for different kinds of tumors, encompassing hepatocellular carcinoma, bladder cancer, and clear cell renal cell carcinoma [25-27]. lncRNAs have demonstrated promising as biological indicators and objectives for cancer detection and intervention. [28]. They also have a major part in regulating the cancerous tendencies of tumor cells [29]. But still, the majority of DRLs are yet unknown and their role in EC prognosis is still unclear. In this work, we tried to create a uterine corpus endometrial cancer risk prediction model in order to explore the connection and its function in tumor immunity and treatment.

Our research determined 524 DRLs; these associated with the general survival of EC cases were filtered out for model construction. Employing LASSO regression analysis, a model of risk scores, which comprises five disulfidptosis-related prognostic lncRNAs was created. More than 500 EC cases were divided into train and test groups to evaluate our model's predictive performance. A high degree of risk scores produced by our predictive model might be a sign of poor PFS and OS. We used five DRLs to build a model for predicting risk in EC patients. Specifically, lncRNAs such as *EMSLR*, *PRDX6-AS1*, *AL359715.3*, *AC103563.9* showed noteworthy expression primarily in patients classified as elevated risk. In contrast, *AC022960.1* displayed significant expression among those classified as diminished risk. Following that, C-index and ROC curves, nomograms as well as their calibration curves were used to confirm the modeling's accuracy, which was all as anticipated. Therefore, our DRLs signature is a trustworthy and accurate prognostic indicator for individuals with EC.

An increasing amount of lncRNAs have been attached to development and progression of tumors lately [30, 31]. These lncRNAs possess a noteworthy influence on drug resistance, cancer cell proliferation, and differentiation, which further impact the initiation, progression, as well as prognosis of cancers [32, 33]. Their potential as biomarkers for tumor prediction has garnered significant interest [34].

In our research, we established a prognostic signature including five DRLs (*PRDX6-AS1*, *EMSLR*, *AL359715.3*, *AC103563.9* and *AC022960.1*) intimately linked to EC patients' overall survival (OS). Remarkably, *EMSLR* is dependent on DNA methyltransferase I, causes transcriptional repression of *LncPRESS1* and is linked to the incursion and phenotype of cancerous cells [35]. *PRDX6*, the closest gene to *PRDX6-AS1*, could significantly enhance non-small cell lung cancer's invasiveness and migration capability from in vitro to in vivo, which is unfavorable for prognosis [36, 37]. However, the roles of *AC022960.1*, *AL359715.3*, and *AC103563.9* are yet unknown, which requires further investigation and validation. Because cancer progression involves many complex processes, we used functional annotation analysis to further explore the molecular pathways associated with DRLs. The findings of GO and KEGG pathways demonstrate that DRLs are related to many biological functions such as receptor-ligand activity, Cell adhesion molecules, Wnt signaling pathway and collagen-containing extracellular matrix. The highly conserved Wnt signaling is a signaling mechanism, which is vital for regulating the process of embryonic development and organs as well as the progression of tumors [38]. Wnt pathway dysregulation has a complicated part in nearly every step of carcinogenesis in a variety of malignancies [39]. Molecules involved in cell adhesion perform a significant part in development of the embryo, immune response, tissue repair, and tumor metastasis [40-42]. Key mediators in the development of cancer include cell-to-cell contacts and cell adhesion, which facilitate the disease's hallmarks, such as immune escape and metastatic spread [43]. As an example, aggressive tumors have a noticeable overexpression of *LICAM*, and suppressing it significantly hinders the development, incursion, and dissemination of stomach cancerous cells [44]. The extracellular matrix, a vital part of the microenvironment of the malignancy, encourages the production of exosomes from tumors, triggering the Notch signaling system in tumors, thereby facilitating the formation of tumors [45]. Furthermore, GSEA analysis elucidated that the cellular processes under the low-risk scores category were more enriched in immune-related courses. We can forecast that EC patients belonging to the high-risk category will possess a notably lower infiltration of immune cells compared to the low-risk part. We further investigated disparities in the immune-related TME.

Immune-related components and cells were expressed differentially in different risk parts, based on our studies about the different surrounding immune-related environments of tumors between various EC patients. In addition to being the product of independent genetic mutation and tumor cell proliferation, tumor formation also arises from the combined activity of the tumor stromal microenvironment around and malignant tumors [46]. In light of the ESTIMATE algorithm, the immunological scores are much higher in those cohorts under low risk compared with the patients who belong to high risk, suggesting a lower infiltration of various immune cells in elevated risk ECs. Except for Macrophages M1, which exhibited a higher rating in the ECs at high risk, regulatory T cells, Neutrophils, and Macrophages M0 showed noticeably decreased outcomes in these ECs. Furthermore, we evaluated immune function metrics across these two groups. Remarkably, of the 29 different types of immunological functions, more than half revealed reduced function scores in ECs at high risk.

Macrophages, MHC class 1, type 1 IFN response, as well as *aDCs* demonstrated particularly higher degree in those patients who belong to high-risk ranges. Crucial for anti-tumor immunity, type 1 interferons also cause cancer cells to multiply indefinitely and produce immune checkpoint receptor ligand characteristics in high expression levels from cancer exosomes, according to recent research[47]. Furthermore, human tumor-associated macrophages (TAM) increase matrix metalloproteinase (MMP) and release epidermal growth factor, both of which promote tumor aggressiveness[48]. Considering these results, we hypothesize that the prognosis will be worse for individuals with EC because of a reduction in the aspect of infiltration and activity of immune cells, and our DRLs model can identify these patients.

Somatic mutation, is one of the main factors causing carcinogenesis and tumor growth[49, 50]. TMB is a crucial biomarker in cancer therapy for predicting OS following immune checkpoint inhibitor treatment[51]. Therefore, our results also suggest that immunotherapy outcomes are positively influenced by a larger TMB in the low-risk samples. To further understand the variations in immune treatment responsiveness between these two groups, we utilized the TIDE algorithm, a computing framework designed for the prediction of immunotherapeutics[52]. The higher TIDE scores, the more likely to develop tumor immune escape and that the sample is not sensitive to immunotherapy. According to the TIDE algorithm's prediction, immunotherapy works better for people with EC who fall into the low-risk category. We therefore thought that the model we created would offer trustworthy biomarkers of immunity in the therapy of cancers. These findings manifested our risk score model's prognostic significance for EC patients who received immunotherapy. As a result, for the purpose of researching the resistance and responsiveness of related chemotherapy drugs, we assessed the anti-cancer medications' sensitivity for various risk categories of EC patients. We calculated the chemotherapy agents' IC50 and found that *ABT737*, *Afuresertib*, *Dabrafenib* and *Navitoclax* may have improved these patients' treatment results in the low-risk group. Instead, *BMS-345541*, *Cisplatin*, *Talazoparib*, and *GDC0810* provided patients in the high-risk category with greater assistance. These discoveries of this study could help direct more focused care for EC patients in the clinic.

5. Conclusions

In brief, we identified lncRNAs associated with disulfidptosis. We developed a prognostic model based on five DRLs that predicts reactions to chemotherapy, targeted treatment, and immunotherapy as well as independently predict overall survival in EC patients and reflect their immunological response in the microenvironment of the tumor. Undeniably, there are certain constraints in our research. Firstly, the TCGA database, on which we relied for our dataset, has the potential to be biased and incomplete. Different results could be obtained if databases from different sources are combined. Secondly, the properties of the five discovered DRLs may be influenced by inter-individual variability among EC patients. Additionally, further investigations are needed to ascertain the particular molecular pathways by which DRLs control the prognosis of EC patients and how they react to anticancer therapies. In order to get over these restrictions and enhance the sta-

bility of our model, new approaches and other research projects will need to be developed.

In comparison with previous studies, what needs to be clarified is as follows. Firstly, our signature established by five DRLs, with fewer and simpler components, is more refined and will partially provide clinicians with clear guidance and appropriate treatment decisions for different EC patients. Secondly, our study has been validated through in vitro studies, and the results proved the accuracy of our signature, which will boost our confidence in the prediction ability of our model. In sum, we are convinced that as medical technology advances, endometrial carcinoma treatment will become more effective and comprehensive.

Abbreviations

UCEC: Uterine corpus endometrial carcinoma; ECs: endometrial carcinoma patients; DRLs: disulfidptosis-related lncRNAs; SLC7A11: Solute carrier family 7, membrane 11; LASSO: Least absolute shrinkage and selection operator; TCGA: The Cancer Genome Atlas; DEGs: Differentially expressed genes; OS: Overall survival; ROC: Receiver operating characteristic; GO: Gene Ontology; KEGG: Kyoto Encyclopedia of Genes and Genomes; PCA: Principal component analysis; AUC: Area under the curve; HR: Hazard ratio; GDSC: Genomics of Drug Sensitivity in Cancer; TME: Tumor Microenvironment; IC50: Half-maximal inhibitory concentration. RT-qPCR: Quantitative Real-time Polymerase Chain Reaction

Conflicts of interest

Every author proclaims that each of them does not have any financial or commercial conflicts to make public in this study.

Consent for publications

The author read and approved the final manuscript for publication.

Ethics Approval

Not applicable.

Data Sharing Declaration

All of the information from the aforementioned studies is available in the database that we used to perform this investigation using open databases: The Cancer Genome Atlas (TCGA, <https://portal.gdc.cancer.gov/>).

Authors' contributions

Each author contributed significantly to the work. SG Z, L H and T L conceived, edited, and examined the paper critically. YX F and YF H completed the analysis of processed data. Together, QQ J and XX gathered and processed the raw data. Every author committed to conception, implementation, data gathering, analysis, and translation, or in each of those areas; they all concurred on the publication where the paper was submitted, they accepted the final version that was published, and they all agreed to accept full responsibility for the effort. Lin Hong, Ya-Xing Fang and Tao Li are co-first authors for this study.

Funding

The funding of this study came from the Natural Science Foundation of Higher Education Institutions of Anhui Province (Grant No. KJ2021A0352), the Research Fund Pro-

ject of Anhui Medical University (Grant No. 2020xkj236).

Acknowledgement

We are grateful to the authors who donated their platforms and contributed their priceless datasets to the TCGA database.

References

1. Trojano G, Olivieri C, Tinelli R, Damiani GR, Pellegrino A, Ciconelli E (2019) Conservative treatment in early stage endometrial cancer: a review. *Acta Biomed* 90 (4): 405-410. doi: 10.23750/abm.v90i4.7800
2. Sorosky JI (2012) Endometrial cancer. *Obstetrics and gynecology* 120 (2 Pt 1): 383-397. doi: 10.1097/AOG.0b013e3182605bf1
3. Urlick ME, Bell DW (2019) Clinical actionability of molecular targets in endometrial cancer. *Nature reviews Cancer* 19 (9): 510-521. doi: 10.1038/s41568-019-0177-x
4. Terzic M, Aimagambetova G, Kunz J, Bapayeva G, Aitbayeva B, Terzic S, Laganà AS (2021) Molecular Basis of Endometriosis and Endometrial Cancer: Current Knowledge and Future Perspectives. *International journal of molecular sciences* 22 (17). doi: 10.3390/ijms22179274
5. Oaknin A, Bosse TJ, Creutzberg CL, Giordano G, Harter P, Joly F, Lorusso D, Marth C, Makker V, Mirza MR, Ledermann JA, Colombo N (2022) Endometrial cancer: ESMO Clinical Practice Guideline for diagnosis, treatment and follow-up. *Annals of oncology : official journal of the European Society for Medical Oncology* 33 (9): 860-877. doi: 10.1016/j.annonc.2022.05.009
6. DeSouza PA, Qu X, Chen H, Patel B, Maher CA, Kim AH (2021) Long, Noncoding RNA Dysregulation in Glioblastoma. *Cancers* 13 (7). doi: 10.3390/cancers13071604
7. Uszczyńska-Ratajczak B, Lagarde J, Frankish A, Guigó R, Johnson R (2018) Towards a complete map of the human long non-coding RNA transcriptome. *Nature reviews Genetics* 19 (9): 535-548. doi: 10.1038/s41576-018-0017-y
8. Blank-Giwojna A, Postepska-Igielska A, Grummt I (2019) lncRNA KHPS1 Activates a Poised Enhancer by Triplex-Dependent Recruitment of Epigenomic Regulators. *Cell reports* 26 (11): 2904-2915.e2904. doi: 10.1016/j.celrep.2019.02.059
9. Statello L, Guo CJ, Chen LL, Huarte M (2021) Gene regulation by long non-coding RNAs and its biological functions. *Nature reviews Molecular cell biology* 22 (2): 96-118. doi: 10.1038/s41580-020-00315-9
10. Ferré F, Colantoni A, Helmer-Citterich M (2016) Revealing protein-lncRNA interaction. *Briefings in bioinformatics* 17 (1): 106-116. doi: 10.1093/bib/bbv031
11. Cai J, Ji Z, Wu J, Chen L, Zheng D, Chen Y, Zhang X, Xie W, Huang J, Chen M, Lin R, Lin W, Chen Y, Li Z (2022) Development and validation of a novel endoplasmic reticulum stress-related lncRNA prognostic signature and candidate drugs in breast cancer. *Frontiers in genetics* 13: 949314. doi: 10.3389/fgene.2022.949314
12. Liu H, Wan J, Chu J (2019) Long non-coding RNAs and endometrial cancer. *Biomedicine & pharmacotherapy = Biomedecine & pharmacotherapie* 119: 109396. doi: 10.1016/j.biopha.2019.109396
13. Zhang HQ, Li T, Li C, Hu HT, Zhu SM, Lu JQ, Chen XJ, Huang HF, Wu YT (2022) LncRNA THOR promotes endometrial cancer progression through the AKT and ERK signaling pathways. *Medical oncology (Northwood, London, England)* 39 (12): 207. doi: 10.1007/s12032-022-01802-z
14. Kim LK, Park SA, Nam EJ, Kim YT, Heo TH, Kim HJ (2023) LncRNA SNHG4 Modulates EMT Signal and Antitumor Effects in Endometrial Cancer through Transcription Factor SP-1. *Biomedicines* 11 (4). doi: 10.3390/biomedicines11041018
15. Zhu CL, Wang Y, Liu Q, Li HR, Yu CM, Li P, Deng XM, Wang JF (2022) Dysregulation of neutrophil death in sepsis. *Frontiers in immunology* 13: 963955. doi: 10.3389/fimmu.2022.963955
16. Liu X, Nie L, Zhang Y, Yan Y, Wang C, Colic M, Olszewski K, Horbath A, Chen X, Lei G, Mao C, Wu S, Zhuang L, Poyurovsky MV, James You M, Hart T, Billadeau DD, Chen J, Gan B (2023) Actin cytoskeleton vulnerability to disulfide stress mediates disulfidoptosis. *Nature cell biology* 25 (3): 404-414. doi: 10.1038/s41556-023-01091-2
17. Yoshihara K, Shahmoradgoli M, Martínez E, Vegesna R, Kim H, Torres-García W, Treviño V, Shen H, Laird PW, Levine DA, Carter SL, Getz G, Stenke-Hale K, Mills GB, Verhaak RG (2013) Inferring tumour purity and stromal and immune cell admixture from expression data. *Nature communications* 4: 2612. doi: 10.1038/ncomms3612
18. Chen B, Khodadoust MS, Liu CL, Newman AM, Alizadeh AA (2018) Profiling Tumor Infiltrating Immune Cells with CIBERSORT. *Methods in molecular biology (Clifton, NJ)* 1711: 243-259. doi: 10.1007/978-1-4939-7493-1_12
19. Mayakonda A, Lin DC, Assenov Y, Plass C, Koeffler HP (2018) Maftools: efficient and comprehensive analysis of somatic variants in cancer. *Genome research* 28 (11): 1747-1756. doi: 10.1101/gr.239244.118
20. Maeser D, Gruener RF, Huang RS (2021) oncoPredict: an R package for predicting in vivo or cancer patient drug response and biomarkers from cell line screening data. *Briefings in bioinformatics* 22 (6). doi: 10.1093/bib/bbab260
21. Geeleher P, Cox NJ, Huang RS (2014) Clinical drug response can be predicted using baseline gene expression levels and in vitro drug sensitivity in cell lines. *Genome biology* 15 (3): R47. doi: 10.1186/gb-2014-15-3-r47
22. Clarke MA, Long BJ, Del Mar Morillo A, Arbyn M, Bakkum-Gomez JN, Wentzensen N (2018) Association of Endometrial Cancer Risk With Postmenopausal Bleeding in Women: A Systematic Review and Meta-analysis. *JAMA internal medicine* 178 (9): 1210-1222. doi: 10.1001/jamainternmed.2018.2820
23. Galluzzi L, Buqué A, Kepp O, Zitvogel L, Kroemer G (2017) Immunogenic cell death in cancer and infectious disease. *Nature reviews Immunology* 17 (2): 97-111. doi: 10.1038/nri.2016.107
24. Qin Y, Liu Y, Xiang X, Long X, Chen Z, Huang X, Yang J, Li W (2023) Cuproptosis correlates with immunosuppressive tumor microenvironment based on pan-cancer multiomics and single-cell sequencing analysis. *Molecular cancer* 22 (1): 59. doi: 10.1186/s12943-023-01752-8
25. Chen H, Yang W, Li Y, Ma L, Ji Z (2023) Leveraging a disulfidoptosis-based signature to improve the survival and drug sensitivity of bladder cancer patients. *Frontiers in immunology* 14: 1198878. doi: 10.3389/fimmu.2023.1198878
26. Wang T, Guo K, Zhang D, Wang H, Yin J, Cui H, Wu W (2023) Disulfidoptosis classification of hepatocellular carcinoma reveals correlation with clinical prognosis and immune profile. *International immunopharmacology* 120: 110368. doi: 10.1016/j.intimp.2023.110368
27. Wang N, Hu Y, Wang S, Xu Q, Jiao X, Wang Y, Yan L, Cao H, Shao F (2024) Development of a novel disulfidoptosis-related lncRNA signature for prognostic and immune response prediction in clear cell renal cell carcinoma. *Scientific reports* 14 (1): 624. doi: 10.1038/s41598-024-51197-2
28. Zhang W, Xie X, Huang Z, Zhong X, Liu Y, Cheong KL, Zhou J, Tang S (2022) The integration of single-cell sequencing, TCGA, and GEO data analysis revealed that PRRT3-AS1 is a biomarker and therapeutic target of SKCM. *Frontiers in immunology* 13:

919145. doi: 10.3389/fimmu.2022.919145
29. Chi Y, Wang D, Wang J, Yu W, Yang J (2019) Long Non-Coding RNA in the Pathogenesis of Cancers. *Cells* 8 (9). doi: 10.3390/cells8091015
 30. Li J, Meng H, Bai Y, Wang K (2016) Regulation of lncRNA and Its Role in Cancer Metastasis. *Oncology research* 23 (5): 205-217. doi: 10.3727/096504016x14549667334007
 31. Seborova K, Vaclavikova R, Rob L, Soucek P, Vodicka P (2021) Non-Coding RNAs as Biomarkers of Tumor Progression and Metastatic Spread in Epithelial Ovarian Cancer. *Cancers* 13 (8). doi: 10.3390/cancers13081839
 32. Cao HL, Liu ZJ, Huang PL, Yue YL, Xi JN (2019) lncRNA-RMRP promotes proliferation, migration and invasion of bladder cancer via miR-206. *European review for medical and pharmacological sciences* 23 (3): 1012-1021. doi: 10.26355/eurrev_201902_16988
 33. Zhang Y, Luo M, Cui X, O'Connell D, Yang Y (2022) Long noncoding RNA NEAT1 promotes ferroptosis by modulating the miR-362-3p/MIOX axis as a ceRNA. *Cell death and differentiation* 29 (9): 1850-1863. doi: 10.1038/s41418-022-00970-9
 34. Han Y, Li X, He F, Yan J, Ma C, Zheng X, Zhang J, Zhang D, Meng C, Zhang Z, Ji X (2019) Knockdown of lncRNA PVT1 Inhibits Glioma Progression by Regulating miR-424 Expression. *Oncology research* 27 (6): 681-690. doi: 10.3727/096504018x15424939990246
 35. Priyanka P, Sharma M, Das S, Saxena S (2022) E2F1-induced lncRNA, EMSLR regulates lncRNA LncPRESS1. *Scientific reports* 12 (1): 2548. doi: 10.1038/s41598-022-06154-2
 36. Li H, Zhang D, Li B, Zhen H, Chen W, Men Q (2021) PRDX6 Overexpression Promotes Proliferation, Invasion, and Migration of A549 Cells in vitro and in vivo. *Cancer management and research* 13: 1245-1255. doi: 10.2147/cmar.S284195
 37. Zhang XX, You JP, Liu XR, Zhao YF, Cui Y, Zhao ZZ, Qi YY (2022) PRDX6 AS1 gene polymorphisms and SLE susceptibility in Chinese populations. *Frontiers in immunology* 13: 987385. doi: 10.3389/fimmu.2022.987385
 38. Xu X, Zhang M, Xu F, Jiang S (2020) Wnt signaling in breast cancer: biological mechanisms, challenges and opportunities. *Molecular cancer* 19 (1): 165. doi: 10.1186/s12943-020-01276-5
 39. Zhou Y, Xu J, Luo H, Meng X, Chen M, Zhu D (2022) Wnt signaling pathway in cancer immunotherapy. *Cancer letters* 525: 84-96. doi: 10.1016/j.canlet.2021.10.034
 40. D'Occhio MJ, Campanile G, Zicarelli L, Visintin JA, Baruselli PS (2020) Adhesion molecules in gamete transport, fertilization, early embryonic development, and implantation-role in establishing a pregnancy in cattle: A review. *Molecular reproduction and development* 87 (2): 206-222. doi: 10.1002/mrd.23312
 41. Duraivelan K, Samanta D (2021) Emerging roles of the nectin family of cell adhesion molecules in tumour-associated pathways. *Biochimica et biophysica acta Reviews on cancer* 1876 (2): 188589. doi: 10.1016/j.bbcan.2021.188589
 42. Ruan Y, Chen L, Xie D, Luo T, Xu Y, Ye T, Chen X, Feng X, Wu X (2022) Mechanisms of Cell Adhesion Molecules in Endocrine-Related Cancers: A Concise Outlook. *Frontiers in endocrinology* 13: 865436. doi: 10.3389/fendo.2022.865436
 43. Läubli H, Borsig L (2019) Altered Cell Adhesion and Glycosylation Promote Cancer Immune Suppression and Metastasis. *Frontiers in immunology* 10: 2120. doi: 10.3389/fimmu.2019.02120
 44. Ichikawa T, Okugawa Y, Toiyama Y, Tanaka K, Yin C, Kitajima T, Kondo S, Shimura T, Ohi M, Araki T, Kusunoki M (2019) Clinical significance and biological role of L1 cell adhesion molecule in gastric cancer. *British journal of cancer* 121 (12): 1058-1068. doi: 10.1038/s41416-019-0646-8
 45. Wu B, Liu DA, Guan L, Myint PK, Chin L, Dang H, Xu Y, Ren J, Li T, Yu Z, Jabban S, Mills GB, Nukpezah J, Chen YH, Furth EE, Gimotty PA, Wells RG, Weaver VM, Radhakrishnan R, Wang XW, Guo W (2023) Stiff matrix induces exosome secretion to promote tumour growth. *Nature cell biology* 25 (3): 415-424. doi: 10.1038/s41556-023-01092-1
 46. Guo C, Zhang W, Zhang Q, Su Y, Hou X, Chen Q, Guo H, Kong M, Chen D (2023) Novel dual CAFs and tumour cell targeting pH and ROS dual sensitive micelles for targeting delivery of paclitaxel to liver cancer. *Artificial cells, nanomedicine, and biotechnology* 51 (1): 170-179. doi: 10.1080/21691401.2023.2193221
 47. Gong W, Donnelly CR, Heath BR, Bellile E, Donnelly LA, Tanner HF, Broses L, Brenner JC, Chinn SB, Ji RR, Wen H, Nör JE, Wang J, Wolf GT, Xie Y, Lei YL (2021) Cancer-specific type-I interferon receptor signaling promotes cancer stemness and effector CD8+ T-cell exhaustion. *Oncoimmunology* 10 (1): 1997385. doi: 10.1080/2162402x.2021.1997385
 48. Aehnlich P, Powell RM, Peeters MJW, Rahbech A, Thor Straten P (2021) TAM Receptor Inhibition-Implications for Cancer and the Immune System. *Cancers* 13 (6). doi: 10.3390/cancers13061195
 49. Huang S (2012) Tumor progression: chance and necessity in Darwinian and Lamarckian somatic (mutationless) evolution. *Progress in biophysics and molecular biology* 110 (1): 69-86. doi: 10.1016/j.pbiomolbio.2012.05.001
 50. Philpott C, Tovell H, Frayling IM, Cooper DN, Upadhyaya M (2017) The NF1 somatic mutational landscape in sporadic human cancers. *Human genomics* 11 (1): 13. doi: 10.1186/s40246-017-0109-3
 51. Addeo A, Friedlaender A, Banna GL, Weiss GJ (2021) TMB or not TMB as a biomarker: That is the question. *Critical reviews in oncology/hematology* 163: 103374. doi: 10.1016/j.critrevonc.2021.103374
 52. Jiang P, Gu S, Pan D, Fu J, Sahu A, Hu X, Li Z, Traugh N, Bu X, Li B, Liu J, Freeman GJ, Brown MA, Wucherpfennig KW, Liu XS (2018) Signatures of T cell dysfunction and exclusion predict cancer immunotherapy response. *Nature medicine* 24 (10): 1550-1558. doi: 10.1038/s41591-018-0136-1